Noname manuscript No.
(will be inserted by the editor)

Shape Optimization of Continua using NURBS as Basis Functions

Hideyuki Azegami · Shota Fukumoto · Taiki Aoyama

Received: date / Accepted: date

Abstract The present paper introduces a numerical solution to shape optimization problems of domains in which boundary value problems of partial differential equations are defined. In the present paper, the finite element method using NURBS as basis functions in the Galerkin method is applied to solve the boundary value problems and to solve a reshaping problem generated by the H1 gradient method for shape optimization, which has been developed as a general solution to shape optimization problems. Numerical examples of linear elastic continua illustrate that this solution works as well as using the conventional finite element method.

Keywords Calculus of variations · Boundary value problem · Shape optimization · Isogeometric analysis · NURBS · H1 gradient method

1 Introduction

Shapes of numerical models in 3D-CAD are defined using non-uniform rational B-spline (NURBS) functions. On the other hand, for solving boundary value problems of partial differential equations, C^0 class functions are used as the basis functions in the standard finite element method. More precisely, polynomials of piecewise lower-order in each finite element and non-smooth between finite elements are used to represent geometric shapes, solution and test functions in the isoparametric finite element method. This difference becomes a serious problem in case slight difference in boundary shape affects on cost functions. Even if in case a finite element model is constructed automatically from a CAD model[37], since the numerical result of the finite element model does not agree with the strict result of the CAD model, this miss match becomes a barrier in analyzing the strict optimal shape.

In order to avoid this miss match, Hughes et al. [18, 13] presented an isogeometric finite element method in which the NURBS functions are used as the basis functions of isoparametric elements in the finite element method. A number of shape optimization methods using the isogeometric finite element model have been proposed. Wall et al. [40] demonstrated the numerical solvability of a shape optimization problem formulated by selecting the coordinates of control points as design variables. They computed derivatives of cost functions with respect to design variables using the chain rule of differentiation and applied a standard optimization algorithm to the subproblem constructed by the obtained derivatives. Cho et al. [11, 14] presented a numerical method for computing the derivatives of cost functions with respect to the coordinates of control points by using the velocity field due to the variation of each control point in the formulae of shape derivatives for domain and boundary integrals. Seo et al. extended the approach of shape optimization by selecting the coordinates of control points as design variables to the topology optimization problem using trimming spline curves[33]. An approach of shape optimization using the boundary integral equation method in isogeometric formulation was presented by Li et al.[27]. Applications of the isogeometric finite element method were presented to vibrating membranes by Manh et al.[28], and to photonic crystals by Qian et al.[42].

This paper was presented in WCSMO-9, Shizuoka.

Hideyuki Azegami · Shota Fukumoto · Taiki Aoyama
Graduate School of Information Science, Nagoya University, A4-2 (780) Furo-cho, Chikusa-ku, Nagoya 464-8601, Japan
Tel.: +81-52-789-4801
Fax: +81-52-789-4801
E-mail: azegami@is.nagoya-u.ac.jp

On the other hand, viewing the shape optimization problem as a nonparametric problem, in which mapping from an initial domain to a new domain is selected as a design variable, the shape optimization problem is found to be irregular because the regularity of the shape derivatives of cost functions with respect to domain variation is less than the regularity required in order to maintain the original regularity of the initial domain[10,38,9,8,46,45,31,16,39,17,15]. In order to compensate for the lack of regularity of the shape derivative, some methods were presented. Mohammadi et al. proposed a method to remake smooth boundary by using the Laplace operator on boundary[29]. Another method introducing the Tikhonov regularization term in cost function was presented by Yamada et al. in the level set approach[43]. Nagy et al. proposed a method using a shape change norm in shape optimization problems of elastic arches[30].

To secure the regularity, another method has been developed by the authors by using the gradient method in Hilbert space $H^1\left(\Omega;\mathbb{R}^d\right)$ for $d \in \{2,3\}$-dimensional domains Ω[2,4,5,22]. In this method, domain variation is obtained as a solution to a boundary value problem of an elliptic partial differential equation, such as a linear elastic problem defined in the original domain using the Neumann condition with the negative value of the shape derivative on the boundary. Since the Neumann condition can be considered as a fictitious traction, we called this method the traction method. This method is similar to methods producing domain variations by fictitious forces[7,44,32]. However, those methods are formulated using parametric design variables of nodal displacements, while the traction method is formulated using non-parametric design variable of domain variation. Moreover, the traction method is basically different from the method using the fictitious linear elastic solution in which the shape derivative is used as the Dirichlet condition[12]. The applications of the traction method to various shape optimization problems in engineering are reported in [34,6,19,24,35,23,36,25,26,20,21]. Moreover, we previously presented a similar method, referred to as the H1 gradient method, for a topology optimization problem of density type[3]. Then, in the context of the H1 gradient method for the topology optimization problem, we refer to the traction method as the H1 gradient method for the shape optimization problem. The definition of the H1 gradient method and the solution obtained using this method are described herein.

Since the H1 gradient method is independent of the numerical method used to solve the boundary value problems, considering the applicability to CAD models, we can choose the isogeometric finite element method to use in solving the boundary value problems. In the present paper, we present a numerical scheme to solve shape optimization problems of linear elastic continua using the isogeometric finite element method and numerical result of the mean compliance minimization problem for an example. By replacing the shape derivative with appropriate ones, the numerical scheme is applicable to various shape optimization problems.

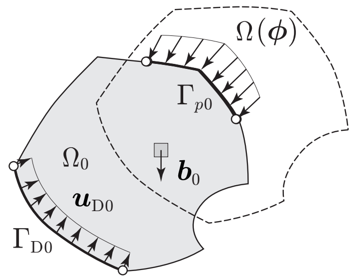

Fig. 1 Initial domain Ω_0 and variation domain $\Omega(\phi)$.

2 Boundary value problem

Let us define an admissible set of design variable and a set of solution to a boundary value problem.

2.1 Initial domain

Let Ω_0 be a $d \in \{2,3\}$-dimensional bounded and fixed domain, as shown in Fig. 1. To define a boundary value problem in Ω_0, its boundary $\partial\Omega_0$ is required at least to be a Lipschitz boundary, i.e. the $W^{1,\infty}$ class. In the present paper, we use the notation $W^{s,p}\left(\Omega_0;\mathbb{R}^d\right)$ as the Sobolev space for the set of functions defined in Ω_0, having value of $\mathbb{R}^d$, and being $s \in [0,\infty]$ times differentiable and $p \in [1,\infty]$-th order Lebesgue integrable, and call its smoothness $W^{s,p}$ class. In the present paper, since we use boundary integral formulae for shape derivatives in Eqs. (7) and (8), we assume the piecewise C^1 class, that is denoted by C^1_{pw} class, for $\partial\Omega_0$ to define the normal $\boldsymbol{\nu}$. We assume that $\Gamma_{\mathrm{D}0} \subset \partial\Omega_0$ is the Dirichlet sub-boundary as $|\Gamma_{\mathrm{D}0}| > 0$, that $\Gamma_{\mathrm{N}0} = \partial\Omega_0 \setminus \bar{\Gamma}_{\mathrm{D}0}$ is the Neumann sub-boundary, and that $\Gamma_{p0} \subset \Gamma_{\mathrm{N}0}$ is the sub-boundary for the nonhomogeneous Neumann condition. In the present paper, we use the $|\cdot|$ notation for domain and boundary as the measure, $\bar{(\cdot)}$ notation as the closure, and $\setminus$ as the set minus operator. Moreover, we assume that Γ_{p0} is of the C^2_{pw} class to define the curvature $\kappa = \boldsymbol{\nabla} \cdot \boldsymbol{\nu}$ in Eq. (7).

2.2 Set of domain mappings

Let $\boldsymbol{\phi} : \Omega_0 \to \mathbb{R}^d$ be the domain variation from the initial domain Ω_0 belonging to $W^{1,\infty}\left(\Omega_0;\mathbb{R}^d\right)$ because of maintaining Lipschitz boundary in new domain, and let

$$\boldsymbol{F}(\boldsymbol{\phi}) = \boldsymbol{\phi}_{\boldsymbol{x}^{\mathrm{T}}} = \left(\frac{\partial \phi_i}{\partial x_j}\right) \in L^{\infty}\left(\Omega_0;\mathbb{R}^{d\times d}\right), \tag{1}$$

$$\omega(\boldsymbol{\phi}) = \det \boldsymbol{F}(\boldsymbol{\phi}) \in L^{\infty}(\Omega_0;\mathbb{R}) \tag{2}$$

be the Jacobi matrix and the Jacobian of $\boldsymbol{\phi}$ with respect to $\boldsymbol{x} \in \Omega_0$, respectively. In the present paper, let $(\cdot)_{\boldsymbol{x}}$ denote $\partial(\cdot)/\partial\boldsymbol{x}$. We define the Banach space for $\boldsymbol{\phi}$ using function composition $\circ$ for addition as follows:

$$\Phi = \Big\{\boldsymbol{\phi} \in W^{1,\infty}\left(\Omega_0;\mathbb{R}^d\right) \;\Big|\; \operatorname*{ess\,inf}_{\boldsymbol{x}\in\Omega_0} \omega(\boldsymbol{\phi}) > 0$$

$$\boldsymbol{\phi} \text{ is } C^1_{\mathrm{pw}} \text{ class on } \partial\Omega_0 \text{ and } C^2_{\mathrm{pw}} \text{ class on } \Gamma_{p0}\Big\}, \tag{3}$$

and the admissible set for $\boldsymbol{\phi}$ as follows:

$$\mathcal{O} = \Big\{\boldsymbol{\phi} \in \Phi \;\Big|\; \|\boldsymbol{\phi} - \boldsymbol{\phi}_0\|_{1,\infty} < 1\Big\},$$

where $\boldsymbol{\phi}_0$ is as identity mapping, e.g., $\boldsymbol{\phi}_0(\boldsymbol{x}) = \boldsymbol{x}$ for $\boldsymbol{x} \in \Omega_0$. $\|\boldsymbol{\phi} - \boldsymbol{\phi}_0\|_{1,\infty} = \|\boldsymbol{\phi} - \boldsymbol{\phi}_0\|_{W^{1,\infty}(\Omega_0;\,\mathbb{R}^d)} < 1$ is used so that $\boldsymbol{\phi} \in \mathcal{O}$ is a one-to-one mapping. We use the notation $\Omega(\boldsymbol{\phi}) = \{\boldsymbol{\phi}(\boldsymbol{x}) \mid \boldsymbol{x} \in \Omega_0,\ \boldsymbol{\phi} \in \mathcal{O}\}$, $\Gamma_p(\boldsymbol{\phi}) = \{\boldsymbol{\phi}(\boldsymbol{x}) \mid \boldsymbol{x} \in \Gamma_{p0},\ \boldsymbol{\phi} \in \mathcal{O}\}$, etc.

2.3 Linear elastic problem

As a boundary value problem, let us consider a linear elastic problem encountered in engineering. Let $D \supset \Omega(\boldsymbol{\phi})$ be a sufficiently large fixed domain, and let $\boldsymbol{b}$, $\boldsymbol{p}$, and $\boldsymbol{u}_{\mathrm{D}}$ be fixed functions as $D \to \mathbb{R}^d$, denoting the body force, traction, and given displacement, respectively. Moreover, let $\boldsymbol{C} : D \to \mathbb{R}^{d\times d\times d\times d}$ be an elliptic, bounded function denoting the stiffness, i.e., there exists $\alpha, \beta > 0$ such that

$$\boldsymbol{\xi} \cdot \boldsymbol{C}\boldsymbol{\xi} \geq \alpha \|\boldsymbol{\xi}\|^2, \quad |\boldsymbol{\xi} \cdot \boldsymbol{C}\boldsymbol{\eta}| \leq \beta \|\boldsymbol{\xi}\| \|\boldsymbol{\eta}\|$$

for all $\boldsymbol{\xi}, \boldsymbol{\eta} \in \left\{\boldsymbol{\xi} \in \mathbb{R}^{d\times d} \;\middle|\; \boldsymbol{\xi} = \boldsymbol{\xi}^{\mathrm{T}}\right\}$ in D. The linear strain and Cauchy stress are denoted as follows:

$$\boldsymbol{E}(\boldsymbol{u}) = \frac{1}{2}\left(\boldsymbol{\nabla}\boldsymbol{u}^{\mathrm{T}} + \left(\boldsymbol{\nabla}\boldsymbol{u}^{\mathrm{T}}\right)^{\mathrm{T}}\right),$$

$$\boldsymbol{T}(\boldsymbol{u}) = \boldsymbol{C}\boldsymbol{E}(\boldsymbol{u}).$$

Let us set $U = H^1\left(\Omega(\boldsymbol{\phi});\mathbb{R}^d\right)$ as the function space for displacement to guarantee existence of an unique solution to weak form of a linear elastic problem using well-suited given functions, $\boldsymbol{\nu}$ as the unit outer normal, and write the linear elastic problem as follows:

Problem 1: Linear elastic problem *For $\boldsymbol{\phi} \in \mathcal{O}$, find $\boldsymbol{u} \in U$ such that*

$$-\boldsymbol{\nabla} \cdot \boldsymbol{T}(\boldsymbol{u}) = \boldsymbol{b}^{\mathrm{T}} \quad \text{in } \Omega(\boldsymbol{\phi}),$$

$$\boldsymbol{T}(\boldsymbol{u})\boldsymbol{\nu} = \boldsymbol{p} \quad \text{on } \Gamma_p(\boldsymbol{\phi}),$$

$$\boldsymbol{T}(\boldsymbol{u})\boldsymbol{\nu} = \boldsymbol{0} \quad \text{on } \Gamma_{\mathrm{N}}(\boldsymbol{\phi}) \setminus \bar{\Gamma}_p(\boldsymbol{\phi}),$$

$$\boldsymbol{u} = \boldsymbol{u}_{\mathrm{D}} \text{ on } \Gamma_{\mathrm{D}}(\boldsymbol{\phi}).$$

Setting the Lagrangian for Problem 1 as

$$\mathscr{L}_{\mathrm{BV}}(\boldsymbol{\phi}, \boldsymbol{u}, \boldsymbol{v}) = \int_{\Omega(\boldsymbol{\phi})} \left(-\boldsymbol{T}(\boldsymbol{u}) \cdot \boldsymbol{E}(\boldsymbol{v}) + \boldsymbol{b} \cdot \boldsymbol{v}\right) \mathrm{d}x$$
$$+ \int_{\Gamma_p(\boldsymbol{\phi})} \boldsymbol{p} \cdot \boldsymbol{v} \;\mathrm{d}\gamma$$
$$+ \int_{\Gamma_{\mathrm{D}}(\boldsymbol{\phi})} \left\{(\boldsymbol{u} - \boldsymbol{u}_{\mathrm{D}}) \cdot \boldsymbol{T}(\boldsymbol{v})\boldsymbol{\nu} + \boldsymbol{v} \cdot \boldsymbol{T}(\boldsymbol{u})\boldsymbol{\nu}\right\} \mathrm{d}\gamma \tag{4}$$

for $\boldsymbol{u}, \boldsymbol{v} \in U$, the solution $\boldsymbol{u}$ to Problem 1 is a stationary point such that

$$\mathscr{L}_{\mathrm{BV}}(\boldsymbol{\phi}, \boldsymbol{u}, \boldsymbol{v}) = 0$$

for all $\boldsymbol{v} \in U$.

3 Shape optimization problem

Let us formulate a shape optimization problem. We call

$$f_0(\boldsymbol{\phi}, \boldsymbol{u}) = -\int_{\Gamma_{\mathrm{D}}(\boldsymbol{\phi})} (\boldsymbol{T}(\boldsymbol{u})\boldsymbol{\nu}) \cdot \boldsymbol{u}_{\mathrm{D}} \;\mathrm{d}\gamma$$
$$+ \int_{\Omega(\boldsymbol{\phi})} \boldsymbol{b} \cdot \boldsymbol{u} \;\mathrm{d}x + \int_{\Gamma_{\mathrm{N}}(\boldsymbol{\phi})} \boldsymbol{p} \cdot \boldsymbol{u} \;\mathrm{d}\gamma \tag{5}$$

the mean compliance and

$$f_1(\boldsymbol{\phi}) = \int_{\Omega(\boldsymbol{\phi})} \mathrm{d}x - c_1 \tag{6}$$

the constraint function for the domain measure, where c_1 is a positive constant such that $f_1(\boldsymbol{\phi}) \leq 0$ for some $\boldsymbol{\phi} \in \mathcal{O}$.

Problem 2: Mean compliance minimization problem *Let $f_0(\boldsymbol{\phi}, \boldsymbol{u})$ and $f_1(\boldsymbol{\phi})$ be as defined in Eqs. (5) and (6), respectively. Find $\boldsymbol{\phi}$, such that*

$$\min_{\boldsymbol{\phi}\in\mathcal{O}} \left\{ f_0(\boldsymbol{\phi}, \boldsymbol{u}) \;\middle|\; f_1(\boldsymbol{\phi}) \leq 0,\ \text{Problem 1}, \boldsymbol{u} \in U \right\}.$$

4 Shape derivative

In order to solve Problem 2 by a gradient-based method, the Fréchet derivatives of the cost functions with respect to the variation of the design variable are required. Let us $\boldsymbol{\varphi}$ denote variation of $\boldsymbol{\phi}$ such that $\boldsymbol{\varphi} \circ \boldsymbol{\phi} \in \mathcal{O}$. In the present paper, we use the $\circ$ notation as $\boldsymbol{\varphi} \circ \boldsymbol{\phi}$ to denote $\boldsymbol{\varphi}(\boldsymbol{\phi}(\boldsymbol{x}))$ for $\boldsymbol{x} \in \Omega_0$. We refer to the Fréchet derivative of $f_0(\boldsymbol{\phi}, \boldsymbol{u})$ with respect to $\boldsymbol{\varphi}$ as the shape derivative of f_0, denoted as $f_0'(\boldsymbol{\phi}, \boldsymbol{u})[\boldsymbol{\varphi}] = \langle \boldsymbol{g}_0, \boldsymbol{\varphi} \rangle$, where $\langle \cdot, \cdot \rangle$ denotes the dual pair. Here, $\boldsymbol{g}_0$ is referred to as the shape gradient for f_0.

Since f_0 is a functional of $\boldsymbol{u}$, Problem 1 becomes a constraint condition for f_0. Then, we define the Lagrangian for f_0 using Eq. (4) as

$$\mathscr{L}_0(\boldsymbol{\phi}, \boldsymbol{u}, \boldsymbol{v}_0) = f_0(\boldsymbol{\phi}, \boldsymbol{u}) + \mathscr{L}_{\mathrm{BV}}(\boldsymbol{\phi}, \boldsymbol{u}, \boldsymbol{v}_0).$$

Here, $\boldsymbol{v}_0 \in U$ is used as the Lagrange multiplier with respect to Problem 1 for f_0. The shape gradient $\boldsymbol{g}_0$ can be obtained using the stationary conditions of $\mathscr{L}_0$. The condition for all variations $\boldsymbol{v}_0' \in U$ of $\boldsymbol{v}_0$, such that

$$\mathscr{L}_{0\boldsymbol{v}_0}(\boldsymbol{\phi}, \boldsymbol{u}, \boldsymbol{v}_0)[\boldsymbol{v}_{0'}] = \mathscr{L}_{\mathrm{BV}\boldsymbol{v}^0}(\boldsymbol{\phi}, \boldsymbol{u}, \boldsymbol{v}_0)[\boldsymbol{v}_0'] = 0$$

is equivalent to the condition that $\boldsymbol{u}$ is the solution to Problem 2.

The stationary condition of $\mathscr{L}_0$ for all variations $\boldsymbol{u}' \in U$ of $\boldsymbol{u}$ such that

$$\begin{aligned}&\mathscr{L}_{0\boldsymbol{u}}(\boldsymbol{\phi}, \boldsymbol{u}, \boldsymbol{v}_0)[\boldsymbol{u}'] \\ &= f_{0\boldsymbol{u}}(\boldsymbol{\phi}, \boldsymbol{u})[\boldsymbol{u}'] + \mathscr{L}_{\mathrm{BV}\boldsymbol{v}}(\boldsymbol{\phi}, \boldsymbol{u}, \boldsymbol{v}_0)[\boldsymbol{u}'] = 0\end{aligned}$$

is equivalent to Problem 3.

Problem 3: Adjoint problem for f_0 *For $\boldsymbol{\phi} \in \mathcal{O}$ and the solution $\boldsymbol{u}$ to Problem 1, find $\boldsymbol{v}_0 \in U$ such that*

$$\begin{aligned}&-\boldsymbol{\nabla} \cdot \boldsymbol{T}(\boldsymbol{v}_0) = \boldsymbol{b}^{\mathrm{T}} \quad \text{in } \Omega(\boldsymbol{\phi}), \\ &\boldsymbol{T}(\boldsymbol{v}_0)\boldsymbol{\nu} = \boldsymbol{p} \quad \text{on } \Gamma_p(\boldsymbol{\phi}), \\ &\boldsymbol{T}(\boldsymbol{v}_0)\boldsymbol{\nu} = \boldsymbol{0} \text{ on } \Gamma_{\mathrm{N}}(\boldsymbol{\phi}) \setminus \Gamma_p(\boldsymbol{\phi}), \\ &\boldsymbol{v}_0 = \boldsymbol{u}_{\mathrm{D}} \quad \text{on } \Gamma_{\mathrm{D}}(\boldsymbol{\phi}).\end{aligned}$$

By comparing Problem 3 with Problem 1, we obtain the self-adjoint relation of $\boldsymbol{v}_0 = \boldsymbol{u}$.

Here, we fix $\boldsymbol{u}$ and $\boldsymbol{v}_0$ with the solutions of Problems 1 and 3. Then, by using the formulae for shape derivatives of domain and boundary integrals[39], we have

$$\begin{aligned}&\mathscr{L}_{0\boldsymbol{\phi}}(\boldsymbol{\phi}, \boldsymbol{u}, \boldsymbol{v}_0)[\boldsymbol{\varphi}] = f_0'(\boldsymbol{\phi}, \boldsymbol{u})[\boldsymbol{\varphi}] \\ &= \int_{\partial\Omega(\boldsymbol{\phi})} \{-\boldsymbol{T}(\boldsymbol{u}) \cdot \boldsymbol{E}(\boldsymbol{v}_0) + \boldsymbol{b} \cdot (\boldsymbol{u} + \boldsymbol{v}_0)\} \boldsymbol{\nu} \cdot \boldsymbol{\varphi} \, \mathrm{d}\gamma \\ &+ \int_{\Gamma_p(\boldsymbol{\phi})} \boldsymbol{p} \cdot \{(\partial_\nu + \kappa)(\boldsymbol{u} + \boldsymbol{v}_0)\} \boldsymbol{\nu} \cdot \boldsymbol{\varphi} \, \mathrm{d}\gamma \\ &+ \int_{\partial\Gamma_p(\boldsymbol{\phi}) \cup \Theta(\boldsymbol{\phi})} \boldsymbol{p} \cdot (\boldsymbol{u} + \boldsymbol{v}_0) \boldsymbol{\tau} \cdot \boldsymbol{\varphi} \, \mathrm{d}a \\ &+ \int_{\Gamma_{\mathrm{D}}(\boldsymbol{\phi})} \big\{\partial_\nu (\boldsymbol{u} - \boldsymbol{u}_{\mathrm{D}}) \cdot \boldsymbol{T}(\boldsymbol{v}_0) \boldsymbol{\nu} \\ &+ \partial_\nu (\boldsymbol{v}_0 - \boldsymbol{u}_{\mathrm{D}}) \cdot \boldsymbol{T}(\boldsymbol{u}) \boldsymbol{\nu}\big\} \boldsymbol{\nu} \cdot \boldsymbol{\varphi} \, \mathrm{d}\gamma \\ &= \langle \boldsymbol{g}_0, \boldsymbol{\varphi} \rangle, \end{aligned} \tag{7}$$

where $\kappa = \boldsymbol{\nabla} \cdot \boldsymbol{\nu}$, $\Theta(\boldsymbol{\phi})$ is the set of non C^1 class points on $\partial\Omega(\boldsymbol{\phi})$, and $\boldsymbol{\tau}$ is the outer tangent of $\Gamma_p(\boldsymbol{\phi}) \setminus \Theta(\boldsymbol{\phi})$, if $d = 3$, at the same time, the normal of $\partial\Gamma_p(\boldsymbol{\phi}) \cup \Theta(\boldsymbol{\phi})$.

For f_1, we have

$$f_1'(\boldsymbol{\phi})[\boldsymbol{\varphi}] = \int_{\partial\Omega(\boldsymbol{\phi})} \boldsymbol{\nu} \cdot \boldsymbol{\varphi} \, \mathrm{d}\gamma = \langle \boldsymbol{g}_1, \boldsymbol{\varphi} \rangle. \tag{8}$$

5 $\boldsymbol{H^1}$ gradient method

The H1 gradient method is proposed as a method for finding the variation of design variable, such as domain variation or density, as a solution to the following problem.

Problem 4: H1 gradient method *Let X be a Hilbert space of H^1 class in which the admissible set of design function is included, and let $b : X \times X \to \mathbb{R}$ be a coercive bilinear form on X such that there exists $\alpha > 0$ that satisfies*

$$a(\boldsymbol{y}, \boldsymbol{y}) \geq \alpha \|\boldsymbol{y}\|_X^2$$

for all $\boldsymbol{y} \in X$. For $\boldsymbol{g}_i \in X'$ (dual space of X) which is a Fréchet derivative of cost function $f_i(\boldsymbol{x})$ at $\boldsymbol{x} \in X$. Find $\boldsymbol{\varphi}_{gi} \in X$ such that

$$a(\boldsymbol{\varphi}_{gi}, \boldsymbol{y}) = -\langle \boldsymbol{g}_i, \boldsymbol{y} \rangle$$

for all $\boldsymbol{y} \in X$.

For the solution $\boldsymbol{\varphi}_{gi} \in X$ to the H1 gradient method, we have the following result.

Theorem 1: H1 gradient method *For $\boldsymbol{g}_i \in X'$, there exists an unique solution $\boldsymbol{\varphi}_{gi} \in X$ to Problem 4. Moreover, the solution $\boldsymbol{\varphi}_{gi}$ decreases f_i.*

Proof: By the Lax-Milgram theorem, there exists an unique solution $\boldsymbol{\varphi}_{gi} \in X$. Moreover, $\boldsymbol{\varphi}_{gi}$ is confirmed to decrease cost function f_i, as follows:

$$\begin{aligned} & f_i(\boldsymbol{x}+\boldsymbol{\varphi}_{gi}) - f_i(\boldsymbol{x}) = \langle \boldsymbol{g}_i, \boldsymbol{\varphi}_{gi} \rangle + o\left(\|\boldsymbol{\varphi}_{gi}\|_X\right) \\ & = -\langle \boldsymbol{\varphi}_{gi}, \boldsymbol{\varphi}_{gi} \rangle + o\left(\|\boldsymbol{\varphi}_{gi}\|_X\right) \\ & \leq -\alpha \|\boldsymbol{\varphi}_{gi}\|_X^2 + o\left(\|\boldsymbol{\varphi}_{gi}\|_X\right). \end{aligned}$$ □

If we assume $\boldsymbol{b} \in L^q\left(D; \mathbb{R}^d\right)$, $\boldsymbol{p} \in W^{1,q}\left(D; \mathbb{R}^d\right)$ and $\boldsymbol{u}_{\mathrm{D}} \in W^{2,q}\left(D; \mathbb{R}^d\right)$ for $q > 2d$, we have that $\boldsymbol{u}$ and $\boldsymbol{v}_0$ belong to $W^{2,q}$ class without singular points such as a crack or $\partial \Gamma_{\mathrm{D}}(\boldsymbol{\phi})$. $W^{2,q}$ class functions are included in the set of the C^1 class functions from the Sobolev embedding theorem. Moreover, since $\partial\Omega(\boldsymbol{\phi})$ is $W^{1,\infty}$ and C^1_{pw} class, $\boldsymbol{\nu}$ is L^∞ and C^0_{pw} class. Also, since Γ_{p0} is C^2_{pw} class, κ is L^∞ and C^0_{pw} class. Then, $\boldsymbol{g}_0$ and $\boldsymbol{g}_1$ in Eqs. (7) and (8), respectively, belong to L^∞ and C^0_{pw} class that is included in X'.

In the shape optimization problem, $H^1\left(\Omega(\boldsymbol{\phi}); \mathbb{R}^d\right)$ is used for X. For the coercive bilinear form of X, we use

$$\begin{aligned} a(\boldsymbol{\varphi}_{gi}, \boldsymbol{y}) &= c_a \int_{\Omega(\boldsymbol{\phi})} \boldsymbol{T}(\boldsymbol{\varphi}_{gi}) \cdot \boldsymbol{E}(\boldsymbol{y})\, \mathrm{d}x \\ &+ \int_{\Gamma_1} \left\{\boldsymbol{\varphi}_{gi} \cdot \boldsymbol{T}(\boldsymbol{y})\boldsymbol{\nu} + \boldsymbol{y} \cdot \boldsymbol{T}(\boldsymbol{\varphi}_{gi})\boldsymbol{\nu}\right\} \mathrm{d}\gamma \end{aligned} \tag{9}$$

in the present paper, where $\Gamma_1 \subset \partial\Omega_0$, $|\Gamma_1| > 0$, is a prescribed sub-boundary on which the boundary variation is fixed, and c_a is a positive constant to control the magnitude of $\boldsymbol{\varphi}_{gi}$ in Problem 4.

The use of this method to solve Problem 2 is described in the next section.

6 Solution to Problem 2

We use the following iterative method based on the sequential quadratic programming to solve Problem 2. In this section, the shape optimization problem is assumed to consist of m constraint functions $f_i \leq 0$ for $i \in \{1, \cdots, m\}$. To determine the domain variation decreasing f_0 while satisfying $f_i \leq 0$ for $i \in \{1, \cdots, m\}$, let us consider the following problem.

Problem 5: SQ approximation *For $\boldsymbol{\phi} \in \mathcal{O}$, let $\boldsymbol{g}_i$ be shape derivatives of f_i for $i \in \{0, \cdots, m\}$, respectively, and $f_i \leq 0$ for $i \in \{1, \cdots, m\}$ are satisfied. Let $a(\,\cdot\,,\,\cdot\,)$ be given as in Eq. (9). Find $\boldsymbol{\varphi}$ such that*

$$\min_{\boldsymbol{\varphi}\circ\boldsymbol{\phi}\in\mathcal{O}} \left\{ q(\boldsymbol{\varphi}) = \frac{1}{2} a(\boldsymbol{\varphi}, \boldsymbol{\varphi}) + \langle \boldsymbol{g}_0, \boldsymbol{\varphi} \rangle \;\middle|\; f_i(\boldsymbol{\phi}, \boldsymbol{u}) + \langle \boldsymbol{g}_i, \boldsymbol{\varphi} \rangle \leq 0 \text{ for } i \in \{1, \cdots, m\} \right\}.$$

The Lagrangian of Problem 5 is defined as

$$\begin{aligned} & \mathscr{L}_{\mathrm{SQ}}(\boldsymbol{\varphi}, \lambda_1, \cdots, \lambda_m) \\ & = q(\boldsymbol{\varphi}) + \sum_{i\in\{1,\cdots,m\}} \lambda_i \left(f_i(\boldsymbol{\phi}, \boldsymbol{u}) + \langle \boldsymbol{g}_i, \boldsymbol{\varphi} \rangle\right) \end{aligned}$$

where $\lambda_i \in \mathbb{R}$ for $i \in \{1, \cdots, m\}$ are the Lagrange multipliers for the constraints. The Karush–Kuhn–Tucker conditions for Problem 5 are given as

$$a(\boldsymbol{\varphi}, \boldsymbol{y}) + \left\langle \left(\boldsymbol{g}_0 + \sum_{i\in\{1,\cdots,m\}} \lambda_i \boldsymbol{g}_i\right), \boldsymbol{y} \right\rangle = 0, \tag{10}$$

$$f_i(\boldsymbol{\phi}, \boldsymbol{u}) + \langle \boldsymbol{g}_i, \boldsymbol{\varphi} \rangle \leq 0 \text{ for } i \in \{1, \cdots, m\}, \tag{11}$$

$$\lambda_i \left(f_i(\boldsymbol{\phi}, \boldsymbol{u}) + \langle \boldsymbol{g}_i, \boldsymbol{\varphi} \rangle\right) = 0 \text{ for } i \in \{1, \cdots, m\}, \tag{12}$$

$$\lambda_i \geq 0 \text{ for } i \in \{1, \cdots, m\} \tag{13}$$

for all $\boldsymbol{y} \circ \boldsymbol{\phi} \in \mathcal{O}$.

Here, let $\boldsymbol{\varphi}_{gi}$ for $i \in \{0, \cdots, m\}$ be the solutions to Problem 4, and set

$$\boldsymbol{\varphi}_g = \boldsymbol{\varphi}_{g0} + \sum_{i\in\{1,\cdots,m\}} \lambda_i \boldsymbol{\varphi}_{gi}. \tag{14}$$

Then, by putting $\boldsymbol{\varphi}_g$ of Eq. (14) for $\boldsymbol{\varphi}$, Eq. (10) holds. If all of the constraints in Eq. (11) are active, i.e. Eq. (11) holds with the equality, we have

$$\left(\langle \boldsymbol{g}_i, \boldsymbol{\varphi}_{gj} \rangle\right)_{ij} (\lambda_j)_j = -\left(f_i(\boldsymbol{\phi}, \boldsymbol{u}) + \langle \boldsymbol{g}_i, \boldsymbol{\varphi}_{g0} \rangle\right)_i. \tag{15}$$

If $g_1, \cdots, g_m$ are linearly independent, Eq. (15) has a unique solution λ_i for $i \in \{1, \cdots, m\}$. Moreover, if $f_i(\boldsymbol{\phi}, \boldsymbol{u}) = 0$ for $i \in \{1, \cdots, m\}$, we have

$$\left(\langle \boldsymbol{g}_i, \boldsymbol{\varphi}_{gj} \rangle\right)_{ij} (\lambda_j)_j = -\left(\langle \boldsymbol{g}_i, \boldsymbol{\varphi}_{g0} \rangle\right)_i. \tag{16}$$

Since Eq. (16) is independent of the magnitude of $\boldsymbol{\varphi}_{g0}$, $\cdots$, $\boldsymbol{\varphi}_{gm}$, (16) is used in the algorithm shown later for the initial domain Ω_0 that satisfies $f_i(\boldsymbol{\phi}, \boldsymbol{u}) \leq 0$ for $i \in \{1, \cdots, m\}$. For $i \in \{1, \cdots, m\}$ such that $\lambda_i < 0$ in the solution λ_i to Eq. (15) or (16), putting $\lambda_i = 0$, removing the constraint for f_i from Eq. (15) or (16), and resolving them, we have λ_i for $i \in \{1, \cdots, m\}$ satisfying Eq. (10) to (13).

The magnitude of $\boldsymbol{\varphi}_g$, which means the step size for domain variation and is evaluated with $|\boldsymbol{\varphi}_g|_{1,2} = \int_{\Omega(\boldsymbol{\phi})} \boldsymbol{E}(\boldsymbol{\varphi}_g) \cdot \boldsymbol{E}(\boldsymbol{\varphi}_g)\, \mathrm{d}x$, is adjusted by selection of c_a in Eq. (9) using criteria such as Armijo's and Wolfe's criteria ensuring global convergence in the original shape optimization problem[1,41]. Let

$$\mathscr{L}(\boldsymbol{\phi}, \boldsymbol{\lambda}) = f_0(\boldsymbol{\phi}, \boldsymbol{u}) + \sum_{i\in\{1,\cdots,m\}} \lambda_i f_i(\boldsymbol{\phi}, \boldsymbol{u})$$

be the Lagrangian for the original optimization problem, and let λ_i for $i \in \{1, \cdots, m\}$ satisfy Eqs. (11) through (13). A criterion for the maximum limit of $|\boldsymbol{\varphi}_g|_{1,2}$ is given by Armijo's criterion as

$$\mathscr{L}(\boldsymbol{\phi} + \boldsymbol{\varphi}_g, \lambda_1, \cdots, \lambda_m) - \mathscr{L}(\boldsymbol{\phi}, \lambda_1, \cdots, \lambda_m) \leq \xi \left\langle \boldsymbol{g}_0 + \sum_{i \in \{1, \cdots, m\}} \lambda_i \boldsymbol{g}_i, \boldsymbol{\varphi}_g \right\rangle \tag{17}$$

for a constant $\xi \in (0, 1)$. The minimum limit of $|\boldsymbol{\varphi}_g|_{1,2}$ is given by Wolfe's criterion as

$$\mu \left\langle \boldsymbol{g}_0 + \sum_{i \in \{1, \cdots, m\}} \lambda_i \boldsymbol{g}_i, \boldsymbol{\varphi}_g \right\rangle \leq \left\langle \boldsymbol{g}_{0\,\mathrm{new}} + \sum_{i \in \{1, \cdots, m\}} \lambda_{i\,\mathrm{new}} \boldsymbol{g}_{i\,\mathrm{new}}, \boldsymbol{\varphi}_g \right\rangle \tag{18}$$

using a constant μ such that $0 < \xi < \mu < 1$, where $(\cdot)_{\mathrm{new}}$ means the function at $\boldsymbol{\phi} + \boldsymbol{\varphi}_g$.

In order to ensure that $f_i(\boldsymbol{\phi}, \boldsymbol{u}) \leq 0$ for $i \in \{1, \cdots, m\}$ are satisfied at $\boldsymbol{\varphi}_g \circ \boldsymbol{\phi}$, we can add a routine updating λ_i by $\lambda_{i\,\mathrm{new}} = \lambda_i + \delta\lambda_i$ for $i \in \{1, \cdots, m\}$, where $\delta\lambda_i$ for $i \in \{1, \cdots, m\}$ are determined by

$$\left(\langle \boldsymbol{g}_i, \boldsymbol{\varphi}_{gj} \rangle\right)_{ij} (\delta\lambda_j)_j = -\left(f_i(\boldsymbol{\varphi}_g \circ \boldsymbol{\phi})\right)_i, \tag{19}$$

where $\boldsymbol{\varphi}_g$ is of in Eq. (14) using old λ_i for $i \in \{1, \cdots, m\}$.

6.1 Algorithm

Combining the above considerations, we propose the following numerical scheme. Let $f_i(\boldsymbol{\phi}, \boldsymbol{u}) = 0$ for $i \in \{1, \cdots, m\}$ be satisfied for Ω_0.

(i) Set Ω_0, c_a in Eq. (9), initial step size $\epsilon > 0$ for $|\boldsymbol{\varphi}_g|_{1,2}$, ex. $\epsilon = 0.01$, parameters of Armijo's and Wolfe's criteria ξ and μ such that $0 < \xi < \mu < 1$, convergence rate $\epsilon_0 > 0$ for $|\boldsymbol{\varphi}_g|_{1,2}$, ex. $\epsilon_0 = 0.001$, and $k = 0$.

(ii) Compute f_i and $\boldsymbol{g}_i$ for $i \in \{0, \cdots, m\}$ at Ω_0.

(iii) Solve $\boldsymbol{\varphi}_{gi}$ for $i \in \{0, \cdots, m\}$ in Problem 4.

(iv) Solve λ_i for $i \in \{0, \cdots, m\}$ as follows.
  - Compute λ_i for $i \in \{1, \cdots, m\}$ by Eq. (16) at $k = 0$ or Eq. (15) at $k > 0$.
  - If $\lambda_i \geq 0$ for $i \in \{1, \cdots, m\}$ is satisfied, proceed to the next step. Otherwise, remove the constraints f_i such that $\lambda_i < 0$, set $\lambda_i = 0$, and resolve Eq. (16) at $k = 0$ or Eq. (15) at $k > 0$ until $\lambda_i \geq 0$ for $i \in \{1, \cdots, m\}$ is satisfied.

(v) Calculate $\boldsymbol{\varphi}_g$ by Eq. (14). If $k = 0$, modify c_a such that $|\boldsymbol{\varphi}_g|_{1,2} = \epsilon$. Compute f_i for $i \in \{0, \cdots, m\}$ at $\Omega(\boldsymbol{\varphi}_g \circ \boldsymbol{\phi})$.
  - If $f_i \leq 0$ for the constraints such that $\lambda_i > 0$, proceed to the next step.
  - Otherwise, do the following. Set λ_{i0} by λ_i for $i \in \{1, \cdots, m\}$, and $j = 0$. $(*)$ By setting $\lambda_{ij} = 0$ for $\lambda_{ij} < 0$ and removing the constraint f_i from Eq. (19), solve for $\delta\lambda_i$ for $i \in \{1, \cdots, m\}$. Set $\lambda_i = \lambda_{i\,j+1}$ by $\lambda_{ij} + \delta\lambda_i$ for $i \in \{1, \cdots, m\}$. If $f_i \leq 0$ for all $i \in \{1, \cdots, m\}$ is not satisfied, set j with $j + 1$, and return to $(*)$.

(vi) Compute $\boldsymbol{g}_i$ for $i \in \{0, \cdots, m\}$ at $\Omega(\boldsymbol{\varphi}_g \circ \boldsymbol{\phi})$.
  - If Eqs. (17) and (18) hold, proceed to the next step.
  - If Eq. (17) or (18) does not hold, update c_a with a larger or smaller value. Return to (v).

(vii) Let $\boldsymbol{\phi}_{k+1} = \boldsymbol{\varphi}_g \circ \boldsymbol{\phi}_k$, $\Omega_{k+1} = \Omega(\boldsymbol{\phi}_{k+1})$, and $\lambda_{ik} = \lambda_i$ for $i \in \{0, \cdots, m\}$, and judge the terminal condition by $|\boldsymbol{\varphi}_g|_{1,2} \leq \epsilon_0$.
  - If the condition holds, terminate the algorithm.
  - Otherwise, replace $k + 1$ with k and return to (iii).

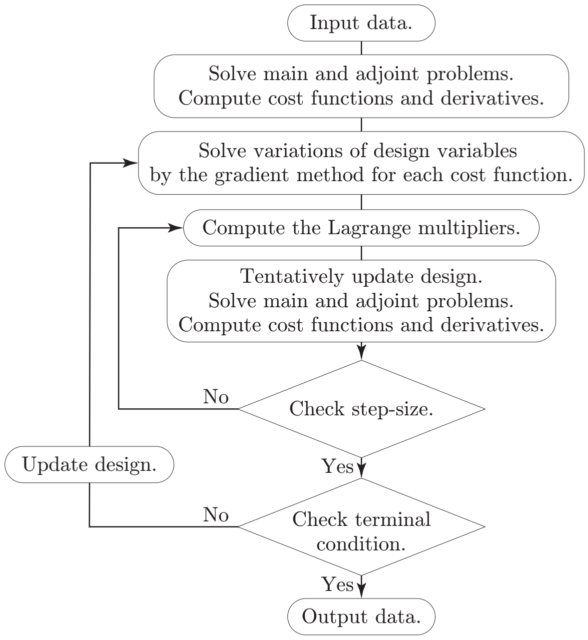

Fig. 2 Schematic flow of algorithm.

In Step (vii), the operation of $\boldsymbol{\phi}_{k+1} = \boldsymbol{\varphi}_g \circ \boldsymbol{\phi}_k$ and $\Omega_{k+1} = \Omega(\boldsymbol{\phi}_{k+1})$ is simple addition of displacements $\boldsymbol{\varphi}_g$ to original domain $\Omega(\boldsymbol{\phi}_k)$. In the isogeometric framework, this operation is performed by moving control point locations. Although this operation is almost equivalent to the case of using control point locations as design variables, the main difference is that the updates of control points are not based on calculation of the sensitivity of the discretized model with respect to control point locations.

7 Isogeometric finite element method

As explained in the introduction, we use the isogeometric finite element method to solve Problems 1, 3, and 4. Let us review the isogeometric finite element method, which is hereinafter used to solve Problem 1. Let

$$\bar{a}\left(\boldsymbol{u}, \boldsymbol{v}\right) = \langle \boldsymbol{l}, \boldsymbol{v} \rangle \tag{20}$$

be the weak form of Problem 1, where

$$\bar{a}\left(\boldsymbol{u}, \boldsymbol{v}\right) = \int_{\Omega(\boldsymbol{\phi})} \boldsymbol{T}\left(\boldsymbol{u}\right) \cdot \boldsymbol{E}\left(\boldsymbol{v}\right) \mathrm{d}x + \int_{\Gamma_{\mathrm{D}}(\boldsymbol{\phi})} \left\{ \boldsymbol{u} \cdot \boldsymbol{T}\left(\boldsymbol{v}\right) \boldsymbol{\nu} + \boldsymbol{v} \cdot \boldsymbol{T}\left(\boldsymbol{u}\right) \boldsymbol{\nu} \right\} \mathrm{d}\gamma \tag{21}$$

$$\langle \boldsymbol{l}, \boldsymbol{v} \rangle = \int_{\Omega(\boldsymbol{\phi})} \boldsymbol{b} \cdot \boldsymbol{v} \, \mathrm{d}x + \int_{\Gamma_p(\boldsymbol{\phi})} \boldsymbol{p} \cdot \boldsymbol{v} \, \mathrm{d}\gamma. \tag{22}$$

7.1 NURBS basic function

For $k, n \in \mathbb{N}$ and $\xi_1, \cdots, \xi_{n+k+1} \in \mathbb{R}$, $\xi_i \leq \xi_{i+1}$, we refer to $b_{i,k} : [\xi_i, \xi_{i+k}] \to \mathbb{R}$ such that

$$b_{i,0}\left(\xi\right) = \begin{cases} 1 \text{ for } \xi \in [\xi_i, \xi_{i+1}) \\ 0 \text{ for } \xi \notin [\xi_i, \xi_{i+1}) \end{cases},$$

$$b_{i,p}i\left(\xi\right) = \frac{\xi - \xi_i}{\xi_{i+p} - \xi_i} b_{i,p-1}\left(\xi\right) + \frac{\xi_{i+p+1} - \xi}{\xi_{i+p+1} - \xi_{i+1}} b_{i+1,p-1}\left(\xi\right)$$

for $p \in \{2, \cdots, k\}$ as the k-th order B-spline basic function. Moreover, for $\boldsymbol{k} \in \mathbb{N}^d$, $\boldsymbol{n} \in \mathbb{N}^d$, $\xi_{i1}, \cdots, \xi_{i\, n_i+k_i} \in \mathbb{R}$ such that $\xi_{ij} \leq \xi_{i\, j+1}$ for $i \in \{1, \cdots, d\}$, $w_{1,\cdots,1}$, $\cdots$, $w_{n_1+k_1,\cdots,n_d+k_d} \in \mathbb{R}$, we refer to $r_{i_1,\cdots,i_d\, k_1,\cdots,k_d}$: $[\xi_{1\, i_1}, \xi_{1\, i_1+k_1}] \times \cdots \times [\xi_{d\, i_d}, \xi_{d\, i_d+k_d}] \to \mathbb{R}$ such that

$$r_{i_1,\cdots,i_d\, k_1,\cdots,k_d}\left(\boldsymbol{\xi}\right) = \frac{a_{i_1,\cdots,i_d\, k_1,\cdots,k_d}}{\sum_{j_1 \in \{1,\cdots,n_1\}} \cdots \sum_{j_d \in \{1,\cdots,n_d\}} a_{i_1,\cdots,i_d\, k_1,\cdots,k_d}}$$

where

$$a_{i_1,\cdots,i_d\, k_1,\cdots,k_d} = b_{i_1,k_1}\left(\xi_1\right) \cdots b_{i_d,k_d}\left(\xi_d\right) w_{i_1,\cdots,i_d}$$

as the d-dimensional NURBS basic function for $\boldsymbol{\xi} \in [\xi_{1i_1}, \xi_{1\, i_1+k_1}] \times \cdots \times [\xi_{di_d}, \xi_{d\, i_d+k_d}]$.

7.2 Isoparametric approximation

Let Ω_h be a finite element approximation of Ω. As in the formulation of isoparametric finite element, setting

$$\Xi = [\xi_{11}, \xi_{1\, n_1+k_1+1}] \times \cdots \times [\xi_{d1}, \xi_{d\, n_d+k_d+1}],$$

$\boldsymbol{x}_h : \Xi \to \Omega_h$ is a shape approximation function, and $\boldsymbol{u}_h, \boldsymbol{v}_h : \Xi \to \mathbb{R}^d$ are approximation functions for $\boldsymbol{u}, \boldsymbol{v}$, such as

$$\boldsymbol{x}_h\left(\boldsymbol{\xi}\right) = \sum_{i_1 \in \{1,\cdots,n_1\}} \cdots \sum_{i_d \in \{1,\cdots,n_d\}} r_{i_1,\cdots,i_d,k_1,\cdots,k_d}\left(\boldsymbol{\xi}\right) \boldsymbol{x}_{i_1,\cdots,i_d},$$

$$\boldsymbol{u}_h\left(\boldsymbol{\xi}\right) = \sum_{i_1 \in \{1,\cdots,n_1\}} \cdots \sum_{i_d \in \{1,\cdots,n_d\}} r_{i_1,\cdots,i_d,k_1,\cdots,k_d}\left(\boldsymbol{\xi}\right) \boldsymbol{u}_{i_1,\cdots,i_d},$$

$$\boldsymbol{v}_h\left(\boldsymbol{\xi}\right) = \sum_{i_1 \in \{1,\cdots,n_1\}} \cdots \sum_{i_d \in \{1,\cdots,n_d\}} r_{i_1,\cdots,i_d,k_1,\cdots,k_d}\left(\boldsymbol{\xi}\right) \boldsymbol{v}_{i_1,\cdots,i_d},$$

where $\boldsymbol{x}_{i_1,\cdots,i_d}, \boldsymbol{u}_{i_1,\cdots,i_d}, \boldsymbol{v}_{i_1,\cdots,i_d} \in \mathbb{R}^d$ are discretized parameters for $\boldsymbol{x}, \boldsymbol{u}$, and $\boldsymbol{v}$ respectively. Moreover, we have

$$\partial_{\boldsymbol{\xi}} r_{i_1,\cdots,i_d,k_1,\cdots,k_d}\left(\boldsymbol{\xi}\right) = \left(\partial_{\boldsymbol{\xi}} \boldsymbol{x}_h^{\mathrm{T}}\right) \partial_{\boldsymbol{x}} r_{i_1,\cdots,i_d,k_1,\cdots,k_d}\left(\boldsymbol{\xi}\right).$$

Then,

$$\partial_{\boldsymbol{x}} r_{i_1,\cdots,i_d,k_1,\cdots,k_d}\left(\boldsymbol{\xi}\right) = \left(\partial_{\boldsymbol{\xi}} \boldsymbol{x}_h^{\mathrm{T}}\right)^{-1} \partial_{\boldsymbol{\xi}} r_{i_1,\cdots,i_d,k_1,\cdots,k_d}\left(\boldsymbol{\xi}\right) \tag{23}$$

holds, where we refer to $\left(\partial_{\boldsymbol{\xi}} \boldsymbol{x}_h^{\mathrm{T}}\right)^{\mathrm{T}} = \left(\partial x_{hi} / \partial \xi_j\right)_{ij} = \boldsymbol{x}_{h\boldsymbol{\xi}^{\mathrm{T}}}$ as the Jacobi matrix. Following the Galerkin method, we substitute $\boldsymbol{u}_h$ and $\boldsymbol{v}_h$ into Eq. (20) and obtain

$$a\left(\boldsymbol{u}_h, \boldsymbol{v}_h\right) = \sum_{i_1 \in \{1,\cdots,n_1\}} \cdots \sum_{i_d \in \{1,\cdots,n_d\}} \sum_{j_1 \in \{1,\cdots,n_1\}} \cdots \sum_{j_d \in \{1,\cdots,n_d\}} \boldsymbol{v}_{i_1,\cdots,i_d} \cdot \left(\int_{\Xi} \boldsymbol{T}\left(r_{i_1,\cdots,i_d,k_1,\cdots,k_d}\left(\boldsymbol{\xi}\right)\right) \cdot \boldsymbol{E}\left(r_{j_1,\cdots,j_d,k_1,\cdots,k_d}\left(\boldsymbol{\xi}\right)\right) \omega_h\left(\boldsymbol{\xi}\right) \mathrm{d}\xi \right) \boldsymbol{u}_{j_1,\cdots,j_d}, \tag{24}$$

$$\langle \boldsymbol{l}, \boldsymbol{v}_h \rangle = \sum_{i_1 \in \{1,\cdots,n_1\}} \cdots \sum_{i_d \in \{1,\cdots,n_d\}} \boldsymbol{v}_{i_1,\cdots,i_d} \cdot \left(\int_{\Xi} r_{i_1,\cdots,i_d,k_1,\cdots,k_d}\left(\boldsymbol{\xi}\right) \boldsymbol{b} \omega_h\left(\boldsymbol{\xi}\right) \mathrm{d}\xi + \int_{\partial \Xi_p} r_{i_1,\cdots,i_d,k_1,\cdots,k_d}\left(\boldsymbol{\xi}\right) \boldsymbol{p} \varpi_h\left(\boldsymbol{\xi}\right) \mathrm{d}\gamma \right), \tag{25}$$

where $\omega_h\left(\boldsymbol{\xi}\right) = \det \boldsymbol{x}_{h\boldsymbol{\xi}^{\mathrm{T}}}$ and

$$\varpi_h\left(\boldsymbol{\xi}\right) = \omega_h\left(\boldsymbol{\xi}\right) \boldsymbol{\nu}_{\xi} \cdot \left\{ \left(\boldsymbol{x}_{h\boldsymbol{\xi}^{\mathrm{T}}}\right)^{-T} \boldsymbol{\nu} \right\}$$

are Jacobians for domain and boundary measures, $\partial \Xi_p = \{\boldsymbol{\xi} \in \Xi \mid \boldsymbol{x}_h(\boldsymbol{\xi}) \in \Gamma_p\}$, and $\boldsymbol{\nu}_\xi$ is the unit outer normal on $\partial \Xi_p$. Then, by setting

$$\mathbf{u} = \left(u_{1,\cdots,1\,1}, \cdots, u_{1,\cdots,1\,d}, \right.$$
$$\left. \cdots, u_{n_1,\cdots,n_d\,d}, \cdots, u_{n_1,\cdots,n_d\,d}\right)^{\mathrm{T}},$$
$$\mathbf{v} = \left(v_{1,\cdots,1\,1}, \cdots, v_{1,\cdots,1\,d}, \cdots, \right.$$
$$\left. v_{n_1,\cdots,n_d\,1}, \cdots, v_{n_1,\cdots,n_d\,d}\right)^{\mathrm{T}},$$

we obtain the following approximation equation for Eq. (20):

$$\mathbf{v} \cdot \boldsymbol{K}\mathbf{u} = \mathbf{v} \cdot \mathbf{l}, \tag{26}$$

where $\boldsymbol{K}$ and $\mathbf{l}$ are defined according to Eqs. (24) and (25), respectively. Equation (26) is solved under the Dirichlet condition for $\mathbf{u}$ and for all $\mathbf{v}$.

8 Numerical examples

We developed a program for shape optimization problems using the isogeometric finite element method. The results obtained using this program are described hereinafter.

8.1 Plate with a hole in plane stress

First, we analyzed a two-dimensional problem related to a linear eleastic problem presented in [18]. Figure 3 shows the boundary conditions of the linear elastic problem as well as the shape variation. The knot mesh, control points, and basic functions used in this analysis are shown in Fig. 4. Here, a plate with a hole, made of a material having a Poisson's ratio of 0.3, is loaded with uniform traction $\boldsymbol{p}_0$ perpendicularly and $2\boldsymbol{p}_0$ horizontally. We used $k_1 = k_2 = 2$, $n_1 = 4$, $n_2 = 3$, and the data in Figs. 4 and [18]. Figure 5 shows the result for the mean compliance minimization problem of the plate with a hole. The shape gradient $\boldsymbol{g}_0$ became uniform on the boundary of the hole (Fig. 5(b)), and the mean compliance f_0 decreases monotonically when the domain measure constraint of f_1 is satisfied.

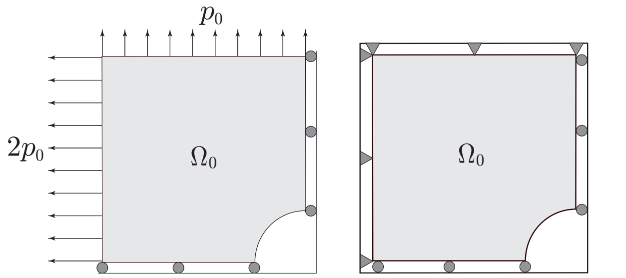

(a) B. C. for Probrem 1 (b) B. C. for Problem 4

Fig. 3 Shape optimization problem of a plate with a hole in plane stress.

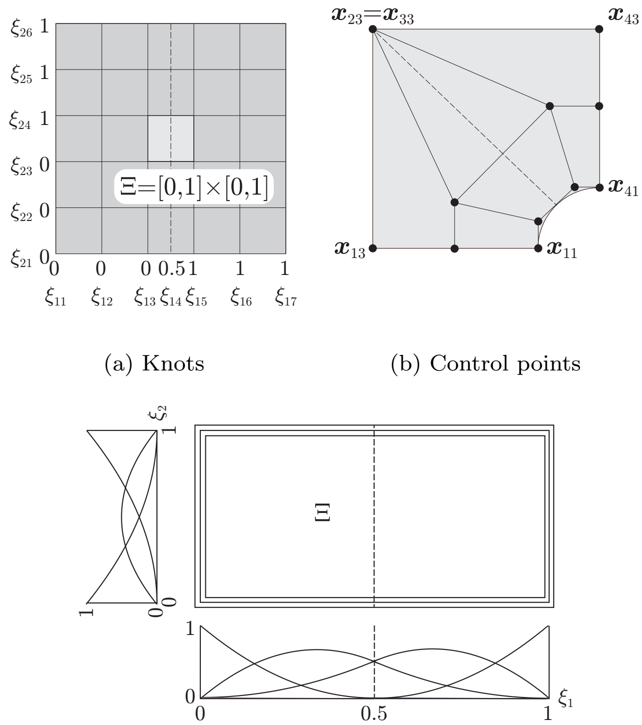

(a) Knots (b) Control points

(c) Basic functions

Fig. 4 Conditions for isogeometric finite element analysis for a plate with a hole.

8.2 Three-dimensional cantilever body

As a three-dimensional problem, we analyzed a three-dimensional cantilever problem. Figure 6 shows settings of the shape optimization problem. A linear elastic body with a Poisson's ratio of 0.3 is loaded by uniform traction $\boldsymbol{p}_0$ perpendicularly in the front plane under a constraint on the back plane. In the shape variation analysis using the H1 gradient method, we assumed the front plane and the center point in the back plane to be fixed, and the back, top, and bottom planes are assumed to be constrained in the normal direction. We analyzed two cases: (1) a knot mesh of $2 \times 2 \times 2$ (Fig. 6 (c)) and $n_1 = n_2 = n_3 = 5$, and (2) a knot mesh of $16 \times 16 \times 16$ (Fig. 6 (d)) and $n_1 = n_2 = n_3 = 19$ using $k_1 = k_2 = k_3 = 3$ and $w_{1,\cdots,1}, \cdots, w_{n_1+k_1,\cdots,n_3+k_3} = 1$. Figures 7 and 8 show the results obtained for Cases (1) and (2), respectively. In both cases, the shape gradi-

(a) $|g_0|$ of initial shape

(b) $|g_0|$ of optimum shape

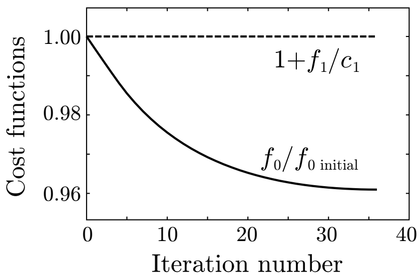

(c) History of cost functions

Fig. 5 Results of Problem 2 for a plate with a hole with $|g_0| = \boldsymbol{T}(\boldsymbol{u}) \cdot \boldsymbol{E}(\boldsymbol{v}_0)$ and history of cost functions. The color indicates the shape derivative $\boldsymbol{g}_0 = g_0\boldsymbol{\nu}$.

ent $\boldsymbol{g}_0$ became uniform on the boundary, and the mean compliance f_0 decreased monotonically when the domain measure constraint of f_1 was satisfied. However, in Case (1), after the shape shown in Fig. 7 (b), unnatural shapes are generated. Observation of the unnatural shapes reveals that the distortion at the wing edges causes an error in the numerical solution to the linear elastic problem, which leads to an error in the shape derivative. On the other hand, since the converging phenomenon occurs in Case (2), the h-refinement of the knot mesh is considered to be as effective as the conventional finite element method for solving the singularity problem (Fig. 9).

9 Conclusion

In the present paper, we presented a numerical solution for shape optimization problems of domains in which the boundary value problems of partial differential equations are defined. To solve the boundary value problems and to solve a reshaping problem constructed by the H1 gradient method for the shape optimization problem, NURBS was used as basis functions in the Galerkin method. The advantage of using the isogeometric finite element method is that there is no mismatch between the design and the evaluation of

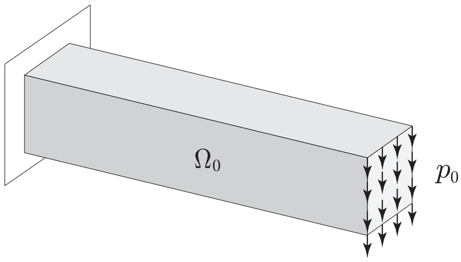

(a) B. C. of the linear elastic problem

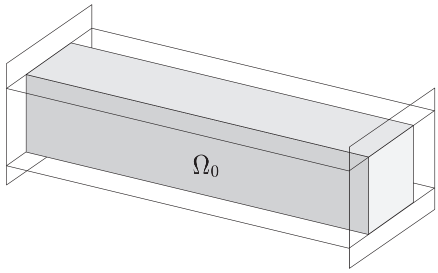

(b) B. C. of shape variation

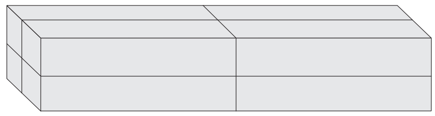

(c) Knot mesh of $2 \times 2 \times 2$

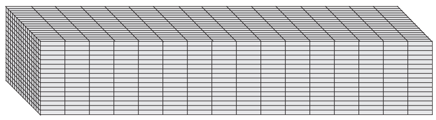

(d) Knot mesh of $16 \times 16 \times 16$

Fig. 6 Shape optimization problem of a three-dimensional cantilever body.

performance. Numerical examples of linear elastic continua indicate that this solution is as appropriate as the solution obtained by the conventional finite element method. Based on the result for the cantilever continuum, h-refinement of the knot mesh is as effective as the conventional finite element method for solving problems involving singularities.

Acknowledgements We want to thank reviewer for their valuable comments. The present study was supported by JSPS KAKENHI (20540113).

References

1. Armijo, L.: Minimization of functions having lipschitz-continuous first partial derivatives. Pacific J. Math. **16**,

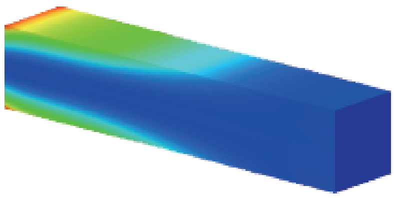

(a) $|g_0|$ of the initial shape

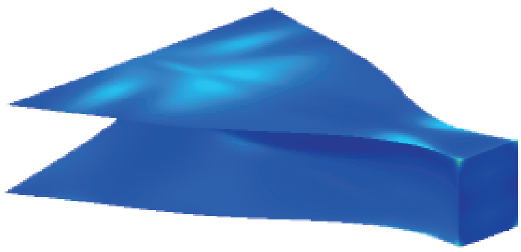

(b) $|g_0|$ of the optimum shape

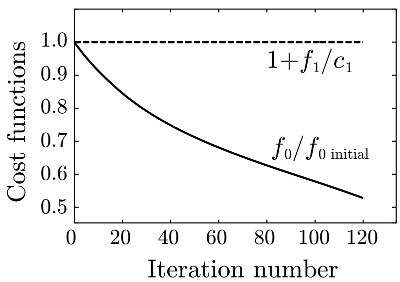

(c) History of cost functions

Fig. 7 Results for a cantilever continuum with $k_1 = k_2 = k_3 = 3$ and a knot mesh of $2 \times 2 \times 2$. The color indicates the shape derivative.

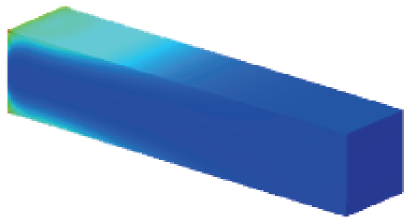

(a) $|g_0|$ of the initial shape

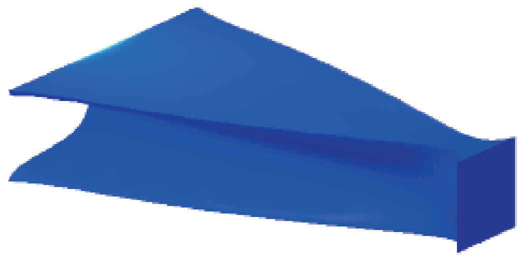

(b) $|g_0|$ of the optimum shape

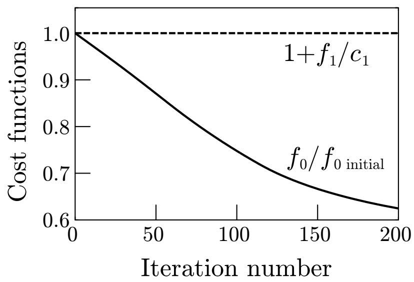

(c) History of cost functions

Fig. 8 Results for a cantilever continuum with $k_1 = k_2 = k_3 = 3$ and a knot mesh of $16 \times 16 \times 16$. The color indicates the shape derivative.

1–3 (1966)
2. Azegami, H.: A solution to domain optimization problems. Trans. of Jpn. Soc. of Mech. Engs., Ser. A **60**, 1479–1486 (1994). (in Japanese)
3. Azegami, H., Kaizu, S., Takeuchi, K.: Regular solution to topology optimization problems of continua. JSIAM Letters **3**, 1–4 (2011)
4. Azegami, H., Shimoda, M., Katamine, E., Wu, Z.C.: A domain optimization technique for elliptic boundary value problems. In: S. Hernandez, M. El-Sayed, C.A. Brebbia (eds.) Computer Aided Optimization Design of Structures IV, Structural Optimization, pp. 51–58. Computational Mechanics Publications, Southampton (1995)
5. Azegami, H., Takeuchi, K.: A smoothing method for shape optimization: traction method using the Robin condition. International Journal of Computational Methods **3**(1), 21–33 (2006)
6. Azegami, H., Yokoyama, S., Katamine, E.: Solution to shape optimization problems of continua on thermal elastic deformation. In: M. Tanaka, G.S. Dulikravich (eds.) Inverse Problems in Engineering Mechanics III, chap. Chap. 2, Sec. 1, pp. 61–66. Elsevier, Tokyo (2002)
7. Belegundu, A.D., Rajan, S.D.: A shape optimization approach based on natural design variables and shape functions. Comput. Meths. Appl. Mech. Engrg. **66**, 87–106 (1988)
8. Cea, J.: Numerical methods of shape optimal design. In: E.J. Haug, J. Cea (eds.) Optimization of Distributed Parameter Structures, vol. 2, pp. 1049–1088. Sijthoff & Noordhoff, Alphen aan den Rijn (1981)
9. Cea, J.: Problems of shape optimization. In: E.J. Haug, J. Cea (eds.) Optimization of Distributed Parameter Structures, vol. 2, pp. 1005–1048. Sijthoff & Noordhoff, Alphen aan den Rijn (1981)
10. Chenais, D.: On the existence of a solution in a domain identification problem. J. of mathematical analysis and applications **52**, 189–219 (1975)
11. Cho, S., Ha, S.H.: Isogeometric shape design optimization: exact geometry and enhanced sensitivity. Struct. Multidisc. Optim. **38**, 53–70 (2009)
12. Choi, K.K., Kim, N.H.: Structural sensitivity analysis and optimization, vol. 1. Springer, New York (2005)
13. Cottrell, J.A., Hughes, T.J.R., Bazilevs, Y.: Isogeometric Analysis Toward Integration of CAD and FEA. Wiley (2009)
14. Ha, S.H., Choi, K.K., Cho, S.: Numerical method for shape optimization using t-spline based isogeometric method. Struct. Multidisc. Optim. **42**, 417–428 (2010)

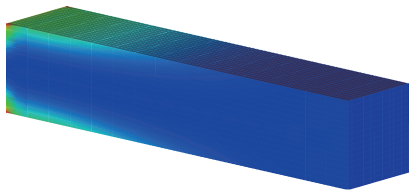

(a) $|g_0|$ of the initial shape

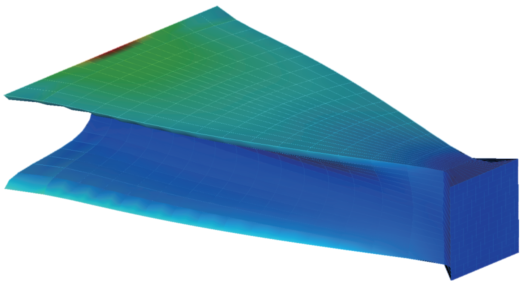

(b) $|g_0|$ of the optimum shape

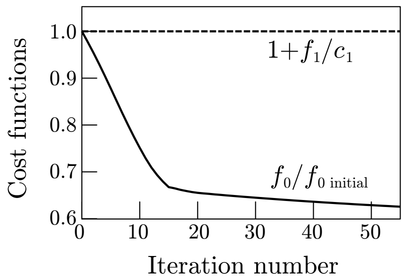

(c) History of cost functions

Fig. 9 Results by FEM for a cantilever continuum with mesh of $16 \times 16 \times 16$. The color indicates the shape derivative.

15. Haslinger, J., Mäkinen, R.A.E.: Introduction to Shape Optimization: Theory, Approximation and Computation. Society for Industrial and Applied Mathematics, Philadelphia (2003)
16. Haslinger, J., Neittaanmäki, P.: Finite Element Approximation for Optimal Shape Design: Theory and Application. John Wiley & Sons, Chichester (1988)
17. Haslinger, J., Neittaanmäki, P.: Finite Element Approximation for Optimal Shape, Material and Topology Design. John Wiley & Sons, Chichester (1996)
18. Hughes, T.J.R., Cottrell, J.A., Bazilevs, Y.: Isogeometric analysis: CAD, finite elements, NURBS, exact geometry and mesh refinement. Comput. Meths. Appl. Mech. Engrg. **194**, 4135–4194 (2005)
19. Inzarulfaisham, A.R., Azegami, H.: Solution to boundary shape optimization problem of linear elastic continua with prescribed natural vibration mode shapes. Structural and Multidisciplinary Optimization **27**(3), 210–217 (2004)
20. Iwai, T., Sugimoto, A., Aoyama, T., Azegami, H.: Shape optimization problem of elastic bodies for controlling contact pressure. JSIAM Letters **2**, 1–4 (2010)
21. Iwata, Y., Azegami, H., Aoyama, T., Katamine, E.: Numerical solution to shape optimization problems for non-stationary navier-stokes problems. JSIAM Letters **2**, 37–40 (2010)
22. Kaizu, S., Azegami, H.: Optimal shape problems and traction method. Transactions of the Japan Society for Industrial and Applied Mathematics **16**(3), 277–290 (2006)
23. Katamine, E., Azegami, H., Hirai, M.: Solution of shape identification problems on thermoelastic solids. International Journal of Computational Methods **3**(3), 279–293 (2006)
24. Katamine, E., Azegami, H., Tsubata, T., Itoh, S.: Solution to shape optimization problems of viscous flow fields. International Journal of Computational Fluid Dynamics **19**(1), 45–51 (2005)
25. Katamine, E., Kawase, Y., Azegami, H.: Shape optimization of thermal forced convection fields. Heat Transfer Asian Research **37**(5), 313–328 (2008)
26. Katamine, E., Nagatomo, Y., Azegami, H.: Shape optimization of 3d viscous flow fields. Inverse Problems in Science and Engineering **17**(1), 105–114 (2009)
27. Li, K., Qian, X.: Isogeometric analysis and shape optimization via boundary integral. Computer-Aided Design **43**, 1427–1437 (2011)
28. Manh, N.D., Evgrafov, A., Gersborg, A.R., Gravesen, J.: Isogeometric shape optimization of vibrating membranes. Comput. Meths. Appl. Mech. Engrg. **200**, 1343–1353 (2011)
29. Mohammadi, B., Pironneau, O.: Applied shape optimization for fluids. Oxford University Press, Oxford, New York (2001)
30. Nagy, A.P., Abdalla, M.M., Gürdal, Z.: Isogeometric design of elastic arches for maximum fundamental frequency. Structural and Multidisciplinary Optimization **43**, 135–149 (2011)
31. Pironneau, O.: Optimal Shape Design for Elliptic Systems. Springer-Verlag, New York (1984)
32. Scherer, M., Denzer, R., Steinmann, P.: A fictitious energy approach for shape optimization. Int. J. Numer. Meth. Engng. **82**, 269–302 (2010)
33. Seo, Y.D., Kim, H.J., Youn, S.K.: Shape optimization and its extension to topological design based on isogeometric analysis. Int. J. Solids Structures **47**, 1618–1640 (2010)
34. Shimoda, M., Azegami, H., Sakurai, T.: Numerical solution for min-max problems in shape optimization: Minimum design of maximum stress and displacement. JSME International Journal Series A **41**(1), 1–9 (1998)
35. Shimoda, M., Tsuji, J., Azegami, H.: Minimum weight shape design for the natural vibration problem of plate and shell structures. In: Hernandez, S., Brebbia, C. A. (eds.) Computer Aided Optimum Design in Engineering IX, pp. 147–156. WIT Press, Southampton, UK (2005)
36. Shimoda, M., Tsuji, J., Azegami, H.: Non-parametric shape optimization method for thin-walled structures under strength criterion. In: S. Hernandez, C.A. Brebbia (eds.) Computer Aided Optimum Design in Engineering X, pp. 179–188. WIT Press, Southampton, UK (2007)
37. Silva, C.A.C., Bittencourt, M.L.: Velocity fields using nurbs with distortion control for structural shape optimization. Structural and Multidisciplinary Optimization **33**, 147–159 (2007)
38. Simon, J.: Differentiation with respect to the domain in boundary value problems. Numerical functional analysis and optimization **2**(7-8), 649–687 (1980)
39. Sokolowski, J., Zolésio, J.P.: Introduction to Shape Optimization: Shape Sensitivity Analysis. Springer-Verlag, New York (1992)

40. Wall, W.A., Frenzel, M.A., Cyron, C.: Isogeometric structural shape optimization. Comput. Meths. Appl. Mech. Engrg. **197**, 2976–2988 (2008)
41. Wolfe, P.: Convergence conditions for ascent methods. SIAM Review **11**, 226–235 (1969)
42. Qian, X., Sigmund, O.: Isogeometric shape optimization of complex geometry via multiple compatible coons patches. Comput. Meths. Appl. Mech. Engrg. **200**, 2237–2255 (2011)
43. Yamada, T., Izui, K., Nishiwaki, S., Takezawa, A.: A topology optimization method based on the level set method incorporating a fictitious interface energy. Comput. Meths. Appl. Mech. Engrg. **199**, 2876–2891 (2010)
44. Yao, T.M., Choi, K.K.: 3-d shape optimal design and automatic finite element regridding. Int. J. Numer. Meth. Engng. **28**, 369–384 (1989)
45. Zolésio, J.P.: Domain variational formulation for free boundary problems. In: E.J. Haug, J. Cea (eds.) Optimization of Distributed Parameter Structures, vol. 2, pp. 1152–1194. Sijthoff & Noordhoff, Alphen aan den Rijn (1981)
46. Zolésio, J.P.: The material derivative (or speed) method for shape optimization. In: E.J. Haug, J. Cea (eds.) Optimization of Distributed Parameter Structures, vol. 2, pp. 1089–1151. Sijthoff & Noordhoff, Alphen aan den Rijn (1981)